Journal of Crystal Growth 346 (2012) 1–4

Contents lists available at SciVerse ScienceDirect

Journal of Crystal Growth

journal homepage: www.elsevier.com/locate/jcrysgro

Growth and characterization of $BaGa_4Se_7$ crystal

Jiyong Yao [a,b], Wenlong Yin [a,b,c], Kai Feng [a,b,c], Xiaomao Li [a,b,c], Dajiang Mei [a,b,c], Qinming Lu [d], Youbao Ni [e], Zhengwei Zhang [f], Zhanggui Hu [a,b], Yicheng Wu [a,b,*]

[a] Center for Crystal Research and Development, Technical Institute of Physics and Chemistry, Chinese Academy of Sciences, Beijing 100190, China
[b] Key Laboratory of Functional Crystals and Laser Technology, Technical Institute of Physics and Chemistry, Chinese Academy of Sciences, Beijing 100190, China
[c] Graduate University of the Chinese Academy of Sciences, Beijing 100049, China
[d] School of Chemistry and Chemistry Engineering, Shan Dong University, Jinan 250100, China
[e] Anhui Institute of Optics and Fine Mechanics, Chinese Academy of Sciences, Hefei 230031, China
[f] Department of Physics, Capital Normal University, Beijing 10048, China

ARTICLE INFO

Article history:
Received 5 December 2011
Received in revised form
19 February 2012
Accepted 22 February 2012
Communicated by R.S. Feigelson
Available online 1 March 2012

Keywords:
A1. Characterization
A1. X-ray diffraction
A2. Bridgman technique
A2. Single crystal growth
B1. Selenides
B2. Nonlinear optic materials

ABSTRACT

High-quality crystals of $BaGa_4Se_7$, a newly developed IR nonlinear optical (NLO) material, were obtained via the Bridgman–Stockbarger technique. The FWHM of the (002) peak rocking curve is about 0.008° and the transmittance through a polished 2 mm thick (001) plate is around 65% over the wide range of 1–14 μm. Various thermophysical properties were measured on crystals. The thermal expansion behavior in $BaGa_4Se_7$ does not exhibit strong anisotropy with $\alpha_a=9.24\times10^{-6}\,K^{-1}$, $\alpha_b=10.76\times10^{-6}\,K^{-1}$, and $\alpha_c=11.70\times10^{-6}\,K^{-1}$ along the three crystallographic axes. The thermal diffusivity/thermal conductivity coefficients measured at 298 K are $0.50(2)\,mm^2\,s^{-1}/0.74(3)\,W\,m^{-1}\,K^{-1}$, $0.42(3)\,mm^2\,s^{-1}/0.64(4)\,W\,m^{-1}\,K^{-1}$, $0.38(2)\,mm^2\,s^{-1}/0.56(4)\,W\,m^{-1}\,K^{-1}$, along the *a*, *b*, *c* crystallographic axis respectively. In addition, the surface laser damage threshold was measured to be 557 MW/cm^2 using a Nd:YAG (1.064 μm) laser under conditions of 5 ns pulse width, 1 Hz frequency, and $D=0.4$ mm spot size.

1. Introduction

Nowadays, the demand for good IR nonlinear (NLO) crystals has been increasingly urgent as mid-far IR lasers have many important civil and military applications including atmospheric monitoring and laser guidance. At present, the ABC_2 chalcopyrite type $AgGaQ_2$ (Q=S, Se) [1,2] and $ZnGeP_2$ [3] crystals are the commercially available materials for mid-IR nonlinear optics owing to their large NLO coefficients and wide transparent regions in the IR region. However, $AgGaQ_2$ have low laser damage thresholds, whereas $ZnGeP_2$ exhibits strong two-photon absorption of conventional 1 μm laser (Nd:YAG), which severely limits their applications [4]. Extensive efforts have been made to find new IR NLO materials that could overcome the shortcomings of currently used materials [5–16].

Recently, $BaGa_4Se_7$ was reported by our group as a new NLO crystal promising for practical application in the mid-IR spectral range [11]. The crystal belongs to the monoclinic system, space group *Pc*, with $a=7.6252(15)$ Å, $b=6.5114(13)$ Å, $c=14.702(4)$ Å, $\beta=121.24(2)°$, and $Z=2$. According to our preliminary study, $BaGa_4Se_7$ exhibits a powder second harmonic generation (SHG) response that is approximately 2–3 times that of $AgGaS_2$. It has a relatively wide band gap of about 2.64 eV (absorption edge 470 nm), which will be beneficial for improving the laser-induced damage threshold and avoiding the two-photon absorption of conventional 1 μm pumping laser. Besides, it is phase matchable in the entire transparent range (0.47–18 μm) based on theoretical calculations. Shortly after our initial report, Petrov et al. [17] obtained bulk crystals of $BaGa_4Se_7$ by Bridgman–Stockbarger technique and measured the refractive index. The experimental refractive index values proved that $BaGa_4Se_7$ is phase matchable in the IR range. For a thorough evaluation of a NLO material, many physical properties in addition to the refractive index need to be investigated. In this paper, we report our efforts in growth and characterization of $BaGa_4Se_7$ crystals. High-quality $BaGa_4Se_7$ crystals in sizes up to $\Phi20\,mm\times30\,mm$ were obtained via the Bridgman–Stockbarger technique and their physical properties including the transmittance spectrum, thermal expansion coefficients, thermal diffusivity and thermal conductivity coefficients, and the laser damage threshold were measured.

* Corresponding author at: Chinese Academy of Sciences, Technical Institute of Physics and Chemistry, Center for Crystal Research and Development, 29 Zhongguancun Dong Lu, Beijing 100190, China.
E-mail address: ycwu@mail.ipc.ac.cn (Y. Wu).

0022-0248/$ - see front matter © 2012 Elsevier B.V. All rights reserved.
doi:10.1016/j.jcrysgro.2012.02.035

2. Experimental section

2.1. Synthesis of polycrystalline material

All staring reagents were commercially available and were used without further purification. Pure polycrystalline $BaGa_4Se_7$ was synthesized from the stoichiometric reaction of the constitute elements with a heating profile that was slightly modified based on the report by Petrov et al. [17]. In a typical reaction, 6.866 g Ba (0.05 mol, 99%), 13.945 g Ga (0.2 mol, 99.9999%), and 27.636 g Se (0.35 mol, 99.9999%) were loaded in a fused-silica tube, under an Ar atmosphere in a glove box. The tube was sealed under a 10^{-4} Pa atmosphere and then placed in a computer-controlled furnace. The sample was heated to 1100 °C in 10 h and kept at that temperature for 24 h, and then the furnace was turned off.

The X-ray powder diffraction pattern of the resultant powder sample was recorded at room temperature in the angular range of $2\theta = 10–70^\circ$ with a scan step width of 0.02° and a fixed counting time of 1 s/step using an automated Bruker D8 X-ray diffractometer equipped with a diffracted monochromator set for Cu K_α ($\lambda = 1.5418$ Å) radiation. It was in excellent agreement with the calculated pattern on the basis of the single crystal crystallographic data of $BaGa_4Se_7$ (Fig. 1) without any detectable impurity.

2.2. Crystal growth

Single crystals of $BaGa_4Se_7$ were grown using Bridgman–Stockbarger method with no seed. The as-prepared powder was loaded into a silica ampoule with appropriate shape and size (previously cleaned with 10 wt% NaOH, distilled water, 10 wt% HF, distilled water and acetone, successively) under an Ar atmosphere in a glove box. The conic bottom of the ampoule was used to encourage spontaneous nucleation and propagation of a single grain. The quartz ampoule was sealed under a 10^{-5} Pa atmosphere and then placed in a vertical six-zone furnace. The ampoule was heated to a temperature exceeding the melting point (1020 °C) by 40–50 °C over 12 h, kept at that temperature for 5 h to force mixing and homogenization of the material. Next, different zones were controlled to certain temperatures to get a property temperature gradient, and kept at those temperatures for 10 h. Then the ampoule was slowly moved from the hot zone to the cold zone to initiate crystallization. After complete solidification, the ampoule was slowly cooled to room temperature.

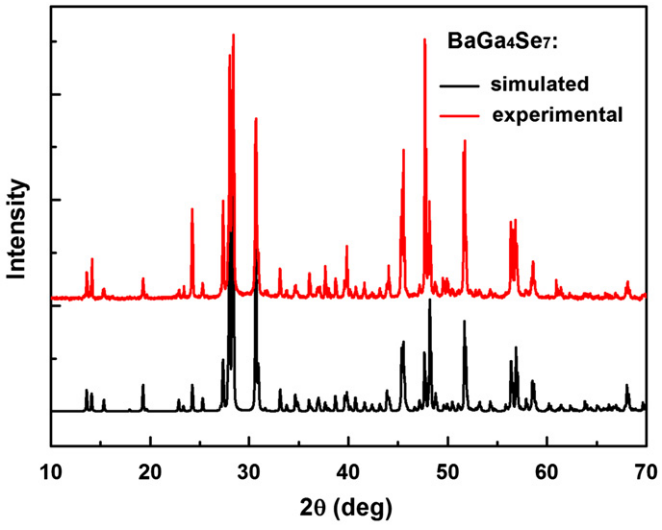

Fig. 1. Experimental (top) and simulated (bottom) X-ray powder diffraction data of $BaGa_4Se_7$.

2.3. Rocking curve measurement

The ω scans around the $BaGa_4Se_7$ (002) diffraction peak with the detector fixed at the 2θ Bragg angle (rocking curve) were performed on a (001) plate.

2.4. Transmission spectrum

A thin (001) plate ($8 \times 5 \times 2$ mm^3) was cut from the as-grown $BaGa_4Se_7$ crystal and polished to optical grades for the optical transmittance measurements without antireflective coating. The transmittance spectrum in the visible and near IR range (0.4–3 μm) was recorded on a Lambda 900UV–vis-NIR (PerkinElmer) and that in the middle IR (2–25 μm) range was measured with the use of a VERTEX 80 V FTIR spectrometer.

2.5. Thermophysical property measurements

The thermal expansion was measured on two rectangular pieces, one with dimensions of $6.32 \times 7.98 \times 5.27$ ($a \times b \times c^*$) mm^3 and the other with dimensions of $5.25 \times 6.01 \times 6.32$ ($a^* \times b \times c$), in the temperature range of 293–573 K under an Ar atmosphere at the heating rate of 5 K min^{-1} with the use of a thermal dilatometer TMA (Perkin-Elmer). The thermal diffusivity and thermal conductivity coefficient along the three crystallographic directions were measured by the laser flash method using a laser flash apparatus (NETZSCHLFA447 Nanoflash) on three plates with the dimensions of about $8 \times 8 \times 2$ mm^3. All plates were coated with gold to enhance the absorption of flash energy and the emission of IR radiation.

2.6. Laser damage threshold

A $8 \times 8 \times 2$ mm^3 $BaGa_4Se_7$ plate with the two surfaces for incidence beam traveling polished was used in the laser damage threshold measurement. The laser source used in this experiment is a commercial pulsed system with a pulse duration of 5 ns and a test repetition rate of 1 Hz at 1064 nm. The beam is focused onto the surface of the sample providing a beam diameter of 0.4 mm. The laser damage test used in this study was the 1-on-1 procedure [18]. Forty sites that were divided into eight fluences by the same energy gap were tested. Each fluence contains five sites. Each site is irradiated by one shot. It can be reckoned, during the test procedure, the irreversible change appeared in surface of the specimen is damage. The pulse fluence which manages to make the corresponding damage probability values of 20% is defined as the laser-induced damage threshold of the specimen herein. As a comparison, we also made measurements of the damage threshold of a high-quality $AgGaS_2$ crystal under the same conditions.

3. Results and discussion

3.1. Crystal growth

Bulk crystals of $BaGa_4Se_7$ were grown by spontaneous crystallization using the Bridgman–Stockbarger technique. After several trials, the temperature gradient in the crystallization zone was chosen to be in the range of 15–23 °C/cm and the growth rate was set in 0.3–0.4 mm/h range. Integral and crack-free $BaGa_4Se_7$ single crystals could be obtained readily. Fig. 2 shows the pictures of an as-grown $BaGa_4Se_7$ crystal with dimensions up to $\Phi 20$ mm × 30 mm, a polished (001) plate and two polished prisms. It can be seen that the crystals are of high quality, which

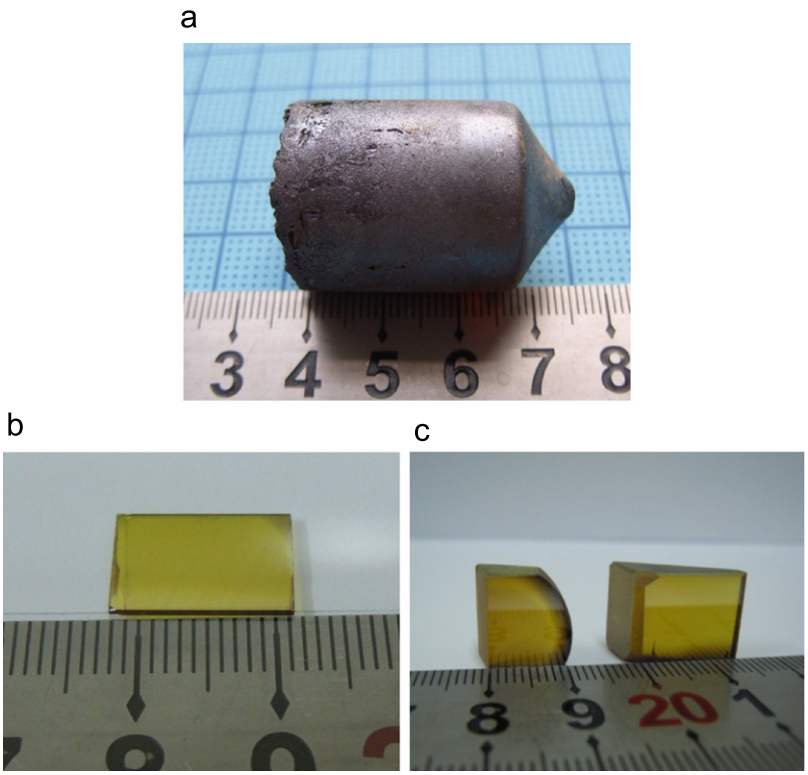

Fig. 2. Photographs of $BaGa_4Se_7$ crystals: (a) $BaGa_4Se_7$ crystal with dimensions of Φ20 mm × 30 mm, (b) transparent (001) pate cut from crystal and (c) two prisms cut from the crystal.

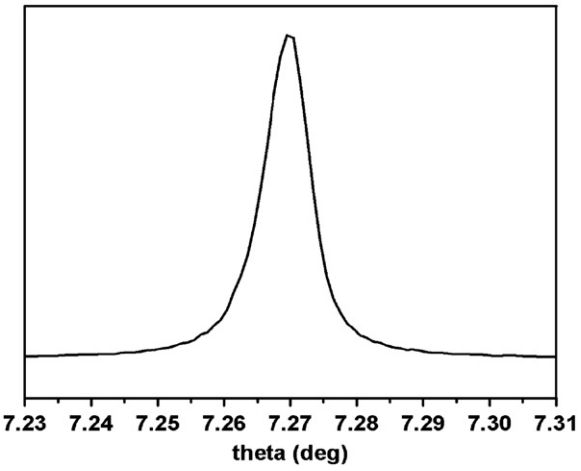

Fig. 3. Rocking curve of the (002) diffraction peak.

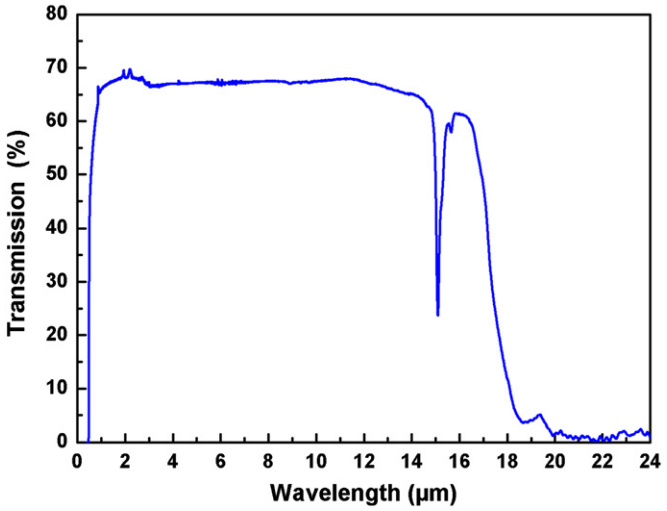

Fig. 4. Transmittance spectrum of $BaGa_4Se_7$ measured on a 2 mm thick (001) plate.

are also confirmed by the following measurements of the (002) peak rocking curve and the transmittance spectrum.

3.2. Rocking curve

Fig. 3 shows the rocking curve for the (002) diffraction peak measured on the (001) plate shown in Fig. 2(b). It exhibits a very small full width at half-maximum (FWHM) of 0.008°, which indicates high crystalline quality of the $BaGa_4Se_7$ crystal.

3.3. Transmission spectrum

As shown in Fig. 4, the $BaGa_4Se_7$ crystal exhibit high transmittance of nearly 65% in the range of 1–14 μm. Considering the refractive loss estimated with Fresnel equation $R=(n-1)^2/(n+1)^2$ (n=refractive index) and the reported refractive index of $BaGa_4Se_7$ [17], this high transmittance is close to the theoretical limit of $(1-R)^2$, which further demonstrate the good quality of the obtained crystal. The absorption edge in the visible range measured on the single crystal is 0.47 μm, which agrees well with our former study using powder diffuse reflectance method. The IR absorption edge is about 18 μm, but there is a strong absorption peak around 15 μm. Although the absorption peak may be related to the two-phonon absorption phenomenon as mentioned in the $AgGaSe_2$ compound, it mechanism may need

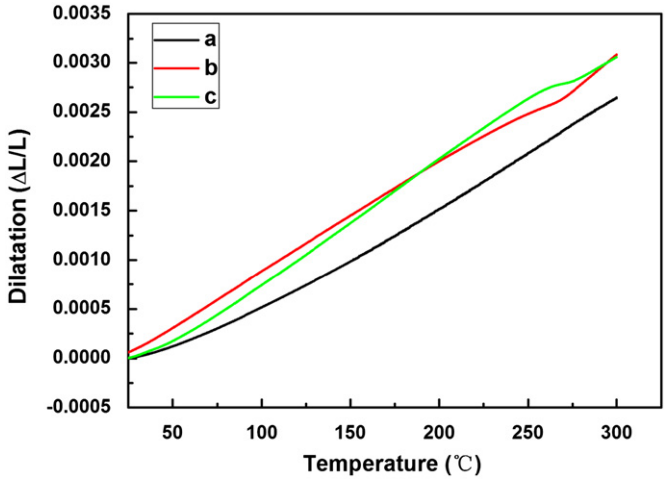

Fig. 5. Thermal expansion along the three crystallographic axes. Dilatation is defined as $\Delta L/L$, where ΔL is the elongation or shrinkage of the sample and L is the length at room temperature.

further investigation. Luckily, the transparent range up to 14 μm is sufficient to cover band II (3–5 μm) and band III (8–14 μm) of atmospheric transparent windows.

3.4. Thermophysical property

The temperature variation of the thermal expansion along the three crystallographic directions is illustrated in Fig. 5. It can be seen that the thermal expansion curves are essentially linear for the three directions in the measured temperature range. The average linear thermal expansion coefficients are all positive with values of $9.24\times10^{-6}\,K^{-1}$, $10.76\times10^{-6}\,K^{-1}$, and $11.70\times10^{-6}\,K^{-1}$ along the *a*, *b*, and *c* directions, respectively, which indicate that the anisotropy in thermal expansion is low for $BaGa_4Se_7$ crystal. Large anisotropic thermal expansion will cause large thermal stress in the crystal during growth and application and thus may lead to crystal cracking. Therefore good optical-quality $BaGa_4Se_7$ is relatively easier to obtain from the point of view of thermal expansion anisotropy. In contrast, the practically used chalcopyrite type IR NLO crystals, $AgGaS_2$ ($12.5\|c$, $-13.8\perp c$) and $AgGaSe_2$ ($16.8\|c$, $-7.8\perp c$) show strong anisotropic thermal expansion, which causes great difficulty in growth of large crystals.

Moreover, the thermal diffusivity coefficients were measured to be $0.50(2)\,mm^2\,s^{-1}$, $0.42(3)\,mm^2\cdot s^{-1}$, and $0.38(2)\,mm^2\,s^{-1}$ at 298 K along the *a*, *b*, and *c* crystallographic axes respectively and the thermal conductivity coefficients were determined as $0.74(3)\,W\,m^{-1}\,K^{-1}$, $0.64(4)\,W\,m^{-1}\,K^{-1}$, $0.56(4)\,W\,m^{-1}\,K^{-1}$ along the *a*, *b*, and *c* directions respectively. The thermal conductivity of $BaGa_4Se_7$ is similar to those of $1.5\,W\,m^{-1}\,K^{-1}$ for $AgGaS_2$ and $1.1\,W\,m^{-1}\,K^{-1}$ for $AgGaSe_2$.

3.5. Laser damage threshold

The experimental results demonstrate that the surface laser damage threshold of $BaGa_4Se_7$ crystal is $557\,MW/cm^2$ at 1.064 μm, 5 ns pulse width, and 1 Hz frequency. In contrast, the referential damage threshold of a high quality $AgGaS_2$ crystal was determined to be about $150\,MW/cm^2$. Our result indicates the $BaGa_4Se_7$ may possess significantly larger laser damage threshold than practically used IR NLO crystal $AgGaS_2$.

4. Conclusion

High-quality crystals of $BaGa_4Se_7$ have been successfully grown via the Bridgman–Stockbarger technique. Based on the transmission spectrum, the crystal exhibits high transmittance over the wide range of 0.47–18 μm, except for an absorption peak at around 15 μm. The thermal expansion coefficients of $BaGa_4Se_7$ were measured to be $\alpha_a=9.24\times10^{-6}\,K^{-1}$, $\alpha_b=10.76\times10^{-6}\,K^{-1}$, and $\alpha_c=11.70\times10^{-6}\,K^{-1}$ along the three crystallographic axes, respectively, which exhibit only weak anisotropy. The thermal diffusivity/thermal conductivity coefficients do not show strong anisotropy along the *a*, *b*, *c* crystallographic axis either. In addition, the surface laser damage threshold was measured to be $557\,MW/cm^2$ (at 1.064 μm, 5 ns pulse width, 1 Hz frequency, and 0.4 mm spot size), which is about 3.7 times that of $AgGaS_2$ crystal measured under identical conditions. Our result indicate the $BaGa_4Se_7$ possess advantages for application in IR NLO optics.

Acknowledgment

This research was supported by National Natural Science Foundation of China (No. 51072203) and the National Basic Research Project of China (No. 2010CB630701).

References

[1] D.S. Chemla, P.J. Kupecek, D.S. Robertson, R.C. Smith, Optics Communication 3 (1971) 29–31.
[2] G.D. Boyd, H.M. Kasper, J.H. McFee, F.G. Storz, IEEE Journal of Quantum Electronics 8 (1972) 900–908.
[3] G.D. Boyd, E. Buehler, F.G. Storz, Applied Physics Letters 18 (1971) 301–304.
[4] P.G. Schunemann, AIP Conference Proceedings 916 (2007) 541–559.
[5] S. Wang, N. Ye, Journal of the American Chemical Society 133 (2011) 11458–11461.
[6] S. Banerjee, C.D. Malliakas, J.I. Jang, J.B. Ketterson, M.G. Kanatzidis, Journal of the American Chemical Society 130 (2008) 12270–12272.
[7] I. Chung, J.H. Song, J.I. Jang, A.J. Freeman, J.B. Ketterson, M.G. Kanatzidis, Journal of the American Chemical Society 131 (2009) 2647–2656.
[8] S.P. Guo, G.C. Guo, M.S. Wang, J.P. Zou, G. Xu, G.J. Wang, X.F. Long, J.S. Huang, Inorganic Chemistry 4 (2009) 7059–7065.
[9] Y. Kim, I.S. Seo, S.W. Martin, J. Baek, P.S. Halasyamani, N. Arumugam, H. Steinfink, Chemistry of Materials 20 (2008) 6048–6052.
[10] X. Lin, G. Zhang, N. Ye, Crystal Growth and Design 9 (2009) 1186–1189.
[11] J.Y. Yao, D.J. Mei, L. Bai, Z.S. Lin, W.L. Yin, P.Z. Fu, Y.C. Wu, Inorganic Chemistry 49 (2010) 9212–9216.
[12] D.J. Mei, W.L. Yin, L. Bai, Z.S. Lin, J.Y. Yao, P.Z. Fu, Y.C. Wu, Dalton Transactions 40 (2011) 3610–3615.
[13] M.C. Chen, L.H. Li, Y.B. Chen, L. Chen, Journal of the American Chemical Society 133 (2011) 4617–4624.
[14] L. Geng, W.-D. Cheng, C.-S. Lin, W.-L. Zhang, H. Zhang, Z.-Z. He, Inorganic Chemistry 50 (2011) 5679–5686.
[15] L. Isaenko, A. Yelisseyev, S. Lobanov, A. Titov, V. Petrov, J.J. Zondy, P. Krinitsin, A. Merkulov, V. Vedenyapin, J. Smirnova, Crystal Research and Technology 38 (2003) 379–387.
[16] T.K. Bera, J.H. Song, A.J. Freeman, J.I. Jang, J.B. Ketterson, M.G. Kanatzidis, Angewandte Chemie International Edition 47 (2008) 7828–7832.
[17] V. Badikov, D. Badikov, G. Shevyrdyaeva, A. Tyazhev, G. Marchev, V. Panyutin, V. Petrov, A. Kwasniewski, Physica Status Solidi Rapid Research Letters 5 (1) (2011) 31–33.
[18] ISO11254-1, 2011.